ADF/cofilin-driven actin dynamics in early events of *Leishmania* cell division

T. V. Satish Tammana[1], Amogh A. Sahasrabuddhe[1], Virendra K. Bajpai[2] and Chhitar M. Gupta[1,*]

[1]Division of Molecular and Structural Biology and [2]Electron Microscopy Unit, Central Drug Research Institute, M.G. Marg, Lucknow 226001, India

*Author for correspondence (drcmg@rediffmail.com)

Accepted 17 March 2010
Journal of Cell Science 123, 1894-1901

doi:10.1242/jcs.068494

Summary

ADF/cofilin is an actin-dynamics-regulating protein that is required for several actin-based cellular processes such as cell motility and cytokinesis. A homologue of this protein has recently been identified in the protozoan parasite *Leishmania*, which has been shown to be essentially required in flagellum assembly and cell motility. However, the role of this protein in cytokinesis remains largely unknown. We show here that deletion of the gene encoding ADF/cofilin in these organisms results in several aberrations in the process of cell division. These aberrations include delay in basal body and kinetoplast separation, cleavage furrow progression and flagellar pocket division. In addition to these changes, the intracellular trafficking and actin dynamics are also adversely affected. All these abnormalities are, however, reversed by episomal complementation. Together, these results indicate that actin dynamics regulates early events in *Leishmania* cell division.

Key words: *Leishmania*, Actin dynamics, Kinetoplast, Basal bodies, Flagellar pocket, Cell division

Introduction

Actin is a highly conserved ubiquitous cytoskeletal protein that is essentially required in several important cellular processes such as cell division, cell motility, intracellular trafficking and endocytosis (Qualmann and Kessels, 2009; Kunda and Baum, 2009). It primarily exists in two forms: the monomeric globular form (G-actin) and the functional filamentous form (F-actin). The dynamics of actin-filament assembly and disassembly is regulated by a specific group of actin-binding proteins of which the actin-depolymerizing factor ADF/cofilin is an important component (Van Troys et al., 2008). ADF/cofilin is present in all eukaryotic organisms and has been implicated in several actin-based cellular activities, such as cell motility and cytokinesis (Ono, 2007; Pollard and Borisy, 2003). The main physiological function of these proteins is to depolymerize actin filaments from their pointed ends, and thereby promote filament dynamics (Carlier et al., 1997). In addition to depolymerization, these proteins also exhibit actin-filament-severing activity, which increases the number of filament positive ends and thereby enhances actin turnover (Van Troys et al., 2008). Higher eukaryotes express several isoforms of ADF/cofilin in a tissue-specific manner, which often have different cellular functions (Van Troys et al., 2008). These proteins have also been identified in a number of lower eukaryotic organisms, such as *Acanthamoeba*, *Dictyostelium*, *Toxoplasma*, *Plasmodium* and *Leishmania* (Blanchoin and Pollard, 1998; Aizawa et al., 1995; Allen et al., 1997; Schuler et al., 2005; Tammana et al., 2008).

Leishmania are an important group of flagellated, protozoan parasites that cause several diseases affecting millions of people worldwide, ranging from relatively mild cutaneous lesions to disfiguring mucocutaneous manifestations and fatal visceral disease (Desjeux, 2004). In these organisms, microtubules, rather than actin microfilaments, cover the inner surface of the plasma membrane enveloping the cell body. A small plasma-membrane invagination, called the flagellar pocket is the only site that is completely free of microtubule cytoskeleton, and therefore, it is the exclusive site where endocytosis and recycling of cell-surface molecules takes place (Gull, 1999).

Leishmania parasites express only one isoform of ADF/cofilin, which is essentially required in flagellar assembly and motility (Tammana et al., 2008). Detailed characterization of *Leishmania* ADF/cofilin (Cof) revealed that it readily binds both the monomeric and filamentous (Kapoor et al., 2008) forms of *Leishmania* actin and also depolymerizes filamentous actin into monomers (Tammana et al., 2008). Furthermore, it displays high nucleotide exchange but weak actin-filament-severing activities (Tammana et al., 2008). As the distributions of Cof and actin in *Leishmania* cells are largely polarized towards the flagellar pocket region where the basal body is located (Tammana et al., 2008), and as the cell division in trypanosomatids is initiated with basal body duplication followed by flagellum formation and flagellar pocket division (Ralston and Hill, 2008), we investigated the role of Cof-driven actin dynamics in *Leishmania* cell division. Results presented here indicate that actin dynamics has an important role in *Leishmania* cell division, especially in basal body separation and flagellar pocket division.

Results

Deletion of *Leishmania COF* gene results in impaired cell division

ADF/cofilins are actin-binding proteins that depolymerize F-actin into actin monomers and consequently enhance the actin dynamics (Ono, 2007). Our earlier studies have shown that deletion of *COF* gene in *Leishmania* promastigotes results in completely immotile, short and stumpy cells with highly reduced flagellar length and severely impaired flagellar beat (Tammana et al., 2008). In addition, we observed decreased growth of the mutant cells compared with wild-type cells in culture (Tammana et al., 2008). A detailed examination of these cultures revealed the presence of significantly higher numbers of dividing cells with two nuclei and two kinetoplasts (2N2K) or two nuclei and one kinetoplast (2N1K) in all the growth phases of $COF^{-/-}$ cells, compared with $COF^{+/+}$ and

COF$^{-/-}$ cells complemented with GFP-Cof (*COF*$^{-/-\text{Comp}}$) (Fig. 1). No multinucleated giant cells were, however, observed in these cultures at any given time. These results strongly suggest that, in addition to its essential role in the flagellar assembly, Cof is also involved in *Leishmania* cell division.

To test this possibility, we analyzed the cell cycle progression of log-phase cells that were synchronized at the G1-S boundary using hydroxyurea (HU). The progression of the cell cycle phases was dissected by flow cytometry at 2 hour intervals after releasing the HU block (Fig. 2, and supplementary material Fig. S1). About 90% of *COF*$^{+/+}$, *COF*$^{-/-\text{Comp}}$ and *COF*$^{-/-}$ cells were arrested at the G1-S boundary by the overnight HU treatment (Fig. 2, and supplementary material Fig. S1). Upon releasing the HU block, the G2-M peak reached a maximum by 4 hours in *COF*$^{+/+}$ (75.5±3.5%; *n*=3), *COF*$^{-/-\text{Comp}}$ (71.6±8.8%; *n*=3) and *COF*$^{-/-}$ cells (83.1±12.2%; *n*=3), in a synchronized manner. A decrease in the G2-M cell number (43.4±5.1%; *n*=3), with concomitant increase in the numbers of G1 phase cells (46.6±1.3%; *n*=3) occurred within 6 hours in synchronized *COF*$^{+/+}$ culture. However, the subsequent progression of cell cycle from G2-M to G1 was significantly delayed in *COF*$^{-/-}$ cells, compared with *COF*$^{+/+}$ cells (Fig. 2). In these cells, the G1 phase (43.8±13.1%; *n*=3) reappeared only after 10 hours, indicating a significant delay in progression of G2-M. However, *GFP-COF* complemented mutant cells showed a pattern that was similar to that observed with *COF*$^{+/+}$ cells, except that an increased number of cells, compared with the wild type, were seen in the S phase of the cell cycle. This increase in S-phase cells could be due to overexpression of the GFP-Cof fusion protein in the mutant cells. The delay in the G2-M phase progression was reproducible in two randomly isolated *COF*$^{-/-}$ clones (see supplementary material Fig. S2).

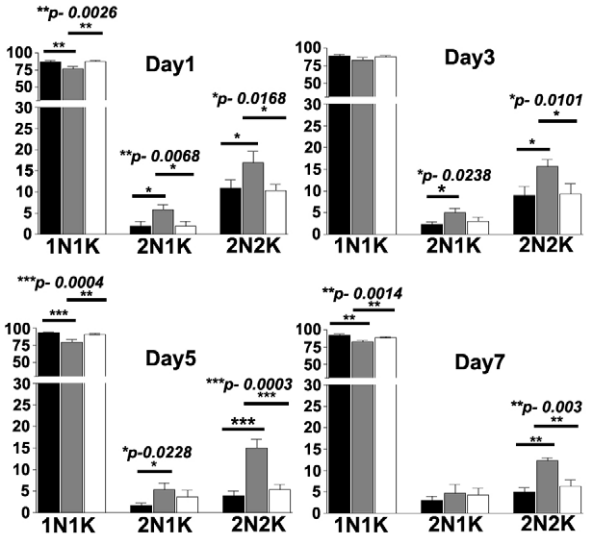

Fig. 1. Cell configurations according to the number of nuclei and kinetoplasts in *Leishmania* *COF*$^{+/+}$ *COF*$^{-/-}$ and *COF*$^{-/-\text{Comp}}$ cells. Cells were counted in *COF*$^{+/+}$ (black bar), *COF*$^{-/-}$ (gray bar) and *COF*$^{-/-\text{Comp}}$ (open bar) cell populations after DAPI staining during different phases of cell growth. 1N1K, cells with single nucleus and single kinetoplast; 2N1K, cells with two nuclei and one kinetoplast; 2N2K, cells with two nuclei and two kinetoplasts. Values are means ± s.d. of three independent experiments. In each experiment, at least 200 cells were analyzed. *P*-values were calculated using one-way analysis of variance and significance among the samples was analyzed by Tukey's multiple comparison test.

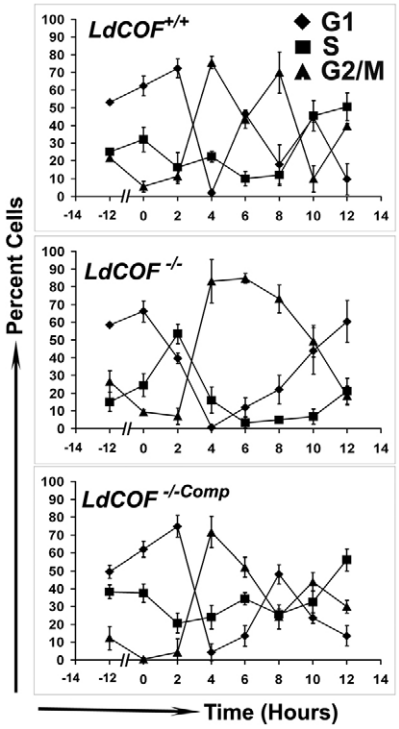

Fig. 2. Cell cycle distribution of *COF*$^{+/+}$, *COF*$^{-/-}$ and *COF*$^{-/-\text{Comp}}$ cells after removing the HU block. The log-phase cells (<10^7/ml) were synchronized at the G1-S border with 200 µg hydroxyurea (HU) for 12 hours. DNA content was measured after staining with propidium iodide (PI) and the cell cycle phases were analyzed by flow cytometry at 2 hour intervals up to 12 hours. The G1, S and G2-M distributions in various cell cycle phases at different time intervals were calculated from the actual data using MOD-FIT software. Before the HU treatment, the characteristic profile of phase distribution observed in all the cell lines was: *COF*$^{+/+}$: G0-G1, 53.1±0.9%; S, 25.0±1.27%; G2-M, 21.7±1.7%; *COF*$^{-/-}$: G0-G1, 58.4±0.7%; S, 15.1±5.4%; G2-M, 26.5±6.0%; *COF*$^{-/-\text{Comp}}$: G0/G1, 49.52±3.75%; S, 38.29±3.9%; G2-M, 12.28±6.45%. The values shown are means ± s.d. of three independent experiments.

Further analysis of the flow cytometry data revealed that *COF*$^{+/+}$ cells returned to the G1 phase by 6 hours, but at this time point, *COF*$^{-/-}$ cells were largely arrested at G2-M. To ascertain whether the observed G2-M arrest was due to delay in mitosis, the *COF*$^{-/-}$ cells were labeled with DAPI 6 hours after HU block and then analyzed for nucleus and kinetoplast division (Fig. 3A). Interestingly, the percentage of 2N2K cells was significantly (*P*=0.009) higher (41.5±6.6%; *n*>600) in *COF*$^{-/-}$ cells, compared with *COF*$^{+/+}$ cells (23±2.6%; *n*>600) and *COF*$^{-/-\text{Comp}}$ cells (27±5.2%; *n*>600), suggesting that the observed G2-M arrest was, in fact, post mitotic.

Cof-null cells show defects in basal body separation and cleavage furrow formation

While observing the status of nuclei and kinetoplasts, it was noticed that the divided kinetoplasts in *COF*$^{-/-}$ cells were more closely positioned to each other than in *COF*$^{+/+}$ and *COF*$^{-/-\text{Comp}}$ cells (Fig. 3B). As the kinetoplasts are physically linked with the basal bodies in trypanosomatids (Robinson et al., 2003), we also analyzed the distances between the basal bodies in the dividing cells. The

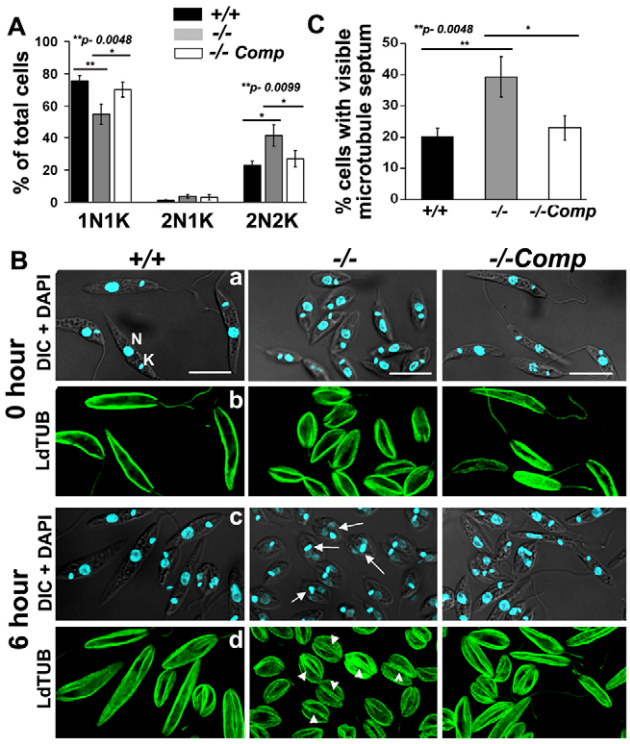

Fig. 3. Analysis of *COF*$^{-/-}$ cells during cytokinetic arrest, compared with *COF*$^{+/+}$ cells and *COF*$^{-/-Comp}$ cells. (**A**) Different cell configurations in *COF*$^{+/+}$ (+/+), *COF*$^{-/-}$ (–/–) and *COF*$^{-/-Comp}$ (–/–Comp) cell types were calculated based on DAPI staining. The values shown are means ± s.d. of three independent experiments. In each experiment, at least 200 cells were analyzed. *P*-values were calculated using one-way analysis of variance and significance among the samples was analyzed by Tukey's multiple comparison test. (**B**) Immunofluorescence images showing the presence of higher numbers of dividing *COF*$^{-/-}$ cells, compared with *COF*$^{+/+}$ and *COF*$^{-/-Comp}$ cells. All cells were treated with HU overnight and the samples were collected at 0 hours and 6 hours after removal of the HU block. The cells were then stained with anti-tubulin antibodies (LdTUB) for visualization of microtubules of cleavage furrow. Interestingly, most of the *COF*$^{-/-}$ cells were arrested during the furrow ingression stage of the cell division. DIC images merged with DAPI (cyan) images showing status of the nucleus and the kinetoplast. LdTUB, *Leishmania* tubulin (green); arrowheads indicate microtubule septa; arrows indicate closely positioned kinetoplasts; DIC, differential interference contrast. Scale bar: 5 µm. (**C**) Percentage of dividing cells with visible microtubule septum in *COF*$^{+/+}$, *COF*$^{-/-}$ and *COF*$^{-/-Comp}$ cell populations, as calculated from immunofluorescence images after staining with anti-tubulin antibodies (LdTUB). The percentage of cells with visible microtubule septum at 6 hours are shown. The values are means ± s.d. of three independent experiments. At least 200 cells in each of three independent experiments were counted. *P*-values were calculated using one-way analysis of variance and significance among the samples was analyzed by Tukey's multiple comparison test.

average distance between the basal bodies, as measured by transmission electron microscopy, in dividing *COF*$^{-/-}$ cells was 118.5±31.3 nm (*n*=10), compared with 184.0±41.5 nm (*n*=4) in *COF*$^{+/+}$ and 164.2±50.8 nm (*n*=4) in *COF*$^{-/-Comp}$ cells. These results indicated that the separation of the divided basal bodies and kinetoplasts was delayed in the dividing *COF*$^{-/-}$ cells. To further explore this problem, we labeled the *COF*$^{+/+}$, *COF*$^{-/-}$ and *COF*$^{-/-Comp}$ cells with anti-tubulin antibodies and then analyzed for the formation of cleavage furrow microtubules at the divisional axis between the daughter cells. About 40% of *COF*$^{-/-}$ cells (39.4±6.5; *n*>600) showed a visible microtubule septum, compared with only ~20% of *COF*$^{+/+}$ (20.3±2.5%; *n*>600) and 23% of *COF*$^{-/-Comp}$ cells (23.0±4.0%; *n*>600) (*P*=0.0048) (Fig. 3C). However, none of the cells showed arrest in the abscission stage, suggesting that the cytokinetic arrest in *COF*$^{-/-}$ cells was upstream of the furrow-ingression stage.

Delayed furrow progression in *COF*$^{-/-}$ cells is caused by abnormalities in flagellar-pocket division and impaired vesicular movement

The events upstream of furrow ingression include the formation of the new flagellum and flagellar-pocket division (Hammarton et al., 2007). As flagellum assembly was severely impaired in *COF*$^{-/-}$ cells (Tammana et al., 2008) and because flagellar biogenesis and flagellar-pocket organization have been shown to be coordinated with cell duplication in trypanosomes (Lacomble et al., 2009; Absalon et al., 2008a), we envisaged that deletion of Cof could affect flagellar-pocket division. In trypanosomatids, flagellar-pocket division starts with an invagination of the flagellar-pocket membrane near the kinetoplast and proceeds towards the cell surface, eventually dividing the pocket into two. To examine flagellar-pocket division in *COF*$^{-/-}$ cells, we labeled the flagellar-pocket membrane with ConA-rhodamine and analyzed the labeled dividing cells using fluorescence microscopy (Fig. 4). About 80% of dividing *COF*$^{+/+}$ cells (81.6±3.5%; *n*>600) and *COF*$^{-/-Comp}$ cells (78.6±4.0%; *n*>600) showed two clearly separated flagellar pockets between the daughter cells. However, in case of *COF*$^{-/-}$ cells, only about 48% (48.0±2.6%; *n*>600) (*P*<0.0001) of dividing cells showed two separated flagellar pockets and the remaining 52% (52.3±2.6%; *n*>600) showed a single flagellar pocket between the daughter cells (Fig. 4A,B; also see supplementary material Fig. S3A), indicating delayed flagellar-pocket division in the mutant cells. Furthermore, in cells where the flagellar pockets were not divided, the two kinetoplasts also appeared closer to each other (Fig. 4A). In the case of *COF*$^{-/-Comp}$ cells, the flagellar pockets and the dividing kinetoplasts were clearly separated.

To further confirm these findings, we analyzed flagellar-pocket division by transmission electron microscopy (Fig. 5). Cross sections through the flagellar pocket region revealed a significantly higher number of *COF*$^{-/-}$ cells with two flagella within the same flagellar pocket (86%, *n*=43) compared with *COF*$^{+/+}$ cells (8%, *n*=50), confirming the delayed flagellar-pocket division in *COF*$^{-/-}$ cells. The flagellar pockets appeared enlarged, and a large number of membrane-bound vesicles were seen to accumulate close to the lumen of the flagellar pocket as well as in the cell body, suggesting disturbances in membrane trafficking in the *COF*$^{-/-}$ cells. To determine whether the flagellar pockets were still functional, we assessed the endocytic activity using the fluorophore N-(3-triethylammoniumpropyl)-4-{6-[4-(diethylamino)phenyl]-hexatrienyl} pyridinium dibromide (FM4-64), which has been widely used as a marker for assessing the flagellar pocket activity in trypanosomatids (Sahin et al., 2008; Mullin et al., 2001). In *Leishmania*, FM4-64 is readily internalized and targeted through endosomes to the final digestive compartment towards the posterior end (Waller and McConville, 2002). In *COF*$^{+/+}$ and *COF*$^{-/-Comp}$ cells, endocytosis of the dye occurred with progressive labeling from flagellar pocket to the posterior end within 120 minutes (Fig. 6). Compared with *COF*$^{+/+}$ cells, the movement of FM4-64 in *COF*$^{-/-}$ cells was significantly slower, because the dye labeling was confined to the flagellar-pocket region for up to 60 minutes and it moved only as far as the kinetoplast and nuclear region by

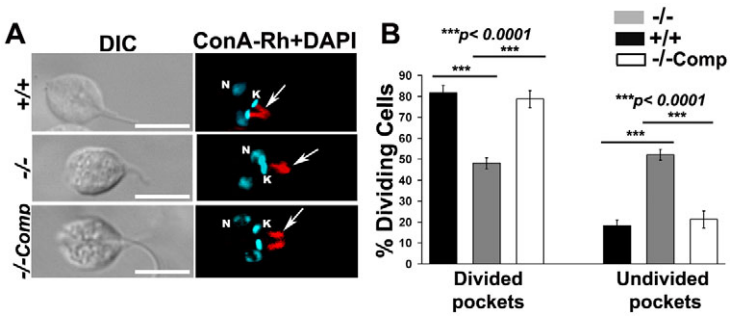

Fig. 4. Delayed flagellar-pocket division. (**A**) Fluorescence images showing two divided flagellar pockets in the $COF^{+/+}$ cells compared with single flagellar pockets in the $COF^{-/-}$ cell population. $COF^{+/+}$, $COF^{-/-}$ and $COF^{-/-Comp}$ cells were fixed with 4% paraformaldehyde in PBS and labeled with ConA-rhodamine (ConA-Rh, red) for flagellar-pocket staining. Nuclei and kinetoplasts are marked by DAPI staining (cyan). The presence of single flagellar pocket in $COF^{-/-}$ cells can be clearly observed compared with two separated flagellar pockets in $COF^{+/+}$ and $COF^{-/-Comp}$ cells. Closely positioned, divided kinetoplasts in the $COF^{-/-}$ cells were also clearly visible. N, nucleus; K, kinetoplast; arrows indicate flagellar pockets. Scale bars: 5 µm. (**B**) Statistical analysis of flagellar pocket status. $COF^{+/+}$, $COF^{-/-}$ and $COF^{-/-Comp}$ cells were counted after labeling their flagellar pockets with ConA-rhodamine. Dividing cells with two clearly separated flagellar pockets were counted under the category of divided pockets and dividing cells with a single flagellar pocket were categorized as undivided pockets. The values shown are means ± s.d. of three independent experiments. At least 200 cells in each of three independent experiments were counted. *P*-values were calculated using one-way analysis of variance and significance among the samples was analyzed by Tukey's multiple comparison test.

120 minutes. Such disturbances in the vesicular movements were also observed in two independently isolated $COF^{-/-}$ clones (see supplementary material Fig. S3B). These results revealed that the intracellular membrane trafficking was adversely affected in $COF^{-/-}$ cells, which, in turn, might have affected flagellar-pocket division and consequently furrow formation.

Impaired vesicular trafficking is linked to the impaired actin dynamics in $COF^{-/-}$ cells

To examine whether altered intracellular vesicular trafficking was associated with the effect of *COF* gene deletion on dynamics of *Leishmania* actin, we analyzed the intracellular distribution of actin in dividing $COF^{-/-}$, $COF^{+/+}$ and $COF^{-/-Comp}$ cells. Actin distribution in $COF^{+/+}$ cells was largely polarized towards the anterior region of the flagellar pocket (Fig. 7, also see supplementary material Fig. S4) and its redistribution occurred only at the later stages of cell division. However, no such polarized actin distribution was seen in the $COF^{-/-}$ cells (Fig. 7). Most of the cellular actin in these cells was sequestered in the form of long cables in the cell body. Furthermore, in more than 90% of dividing $COF^{-/-}$ cells, continuous actin cables were present between the two daughter cells, suggesting an impairment of actin dynamics in these cells. To confirm these findings, we prepared cytoskeletons of $COF^{+/+}$, $COF^{-/-}$ and $COF^{-/-Comp}$ cells using NP-40 (Sahasrabuddhe et al., 2004), and then analyzed them by western blotting and immunofluorescence microscopy (Fig. 8). Anti-GRP78 and anti-PFR antibodies (mAb2E10) were used to label GRP78 (glucose-regulated protein 78, which localizes to the endoplasmic reticulum) and PFR (paraflagellar rod) proteins as detergent-soluble and -insoluble marker proteins, respectively. Densitometric analyses of western blots using anti-actin antibodies revealed that the amount of actin in the detergent-insoluble fraction of $COF^{-/-}$ cells was considerably (P<0.0001) larger (72.1±2.8%; n=3), than in $COF^{+/+}$ (22.6±4.6%; n=3) and $COF^{-/-Comp}$ (49±2.7%; n=3) cells. Further analysis by immunofluorescence microscopy revealed the presence of actin in the flagellar pocket region in the NP-40-treated $COF^{+/+}$ and $COF^{-/-Comp}$ cells, but not in $COF^{-/-}$ cells. Together, these results indicate that the actin dynamics was significantly altered in the $COF^{-/-}$ cells.

Discussion

The present study shows that deletion of the *COF* gene in *Leishmania* results in delayed basal body and kinetoplast separation, as well as in slower division-furrow ingression during cell division. It further reveals that the delayed furrow ingression in mutant cells is caused mainly by the delay in flagellar-pocket division, which is linked to reduced vesicular trafficking and impaired actin dynamics. These results indicate that Cof-driven actin dynamics is required to facilitate various early events underlying *Leishmania* cell division.

Various studies in *Saccharomyces*, *Drosophila*, *Dictyostelium*, *Caenorhabditis* and higher organisms have highlighted the important role of ADF/cofilin in cell survival and cytokinesis. Genetic studies in *Drosophila* show that ADF/cofilin is essential for cytokinesis and centrosome migration (Gunsalus et al., 1995). Furthermore, deletion of the gene encoding cofilin-1 in *Dictyostelium discoideum* leads to cell death, indicating an important role of this protein in cell viability (Aizawa et al., 1995). Similarly, knockdown of the cofilin homologue *UNC-60A* in *Caenorhabditis elegans* causes embryonic lethality with cytokinesis and developmental defects (Ono et al., 2003). In higher organisms, ADF/cofilin is essential for depolymerization of the actin contractile ring that forms between two daughter cells during cell division (Abe et al., 1996). However, in the case of trypanosomatid parasites, cytokinesis is primarily a microtubule-mediated process, and despite the presence of actin and several actin-binding proteins (Sahasrabuddhe et al., 2004; Nayak et al., 2005; Kapoor et al., 2008; Tammana et al., 2008; Katta et al., 2009), their role in these parasites was largely unknown. Our recent studies (Tammana et al., 2008; Sahasrabuddhe et al., 2009) show that the actin-binding proteins Cof and CRN12 have essential roles in flagellar assembly and microtubule remodeling, respectively.

In trypanosomatids, the flagellum emerges from a specialized region called the flagellar pocket, a plasma-membrane invagination, which is also an exclusive site for endocytosis and exocytosis (Morgan et al., 2002a; Morgan et al., 2002b). Several studies have shown that the flagellar-pocket membrane is biochemically distinct from the flagellum or pellicular membrane and is central for trafficking of various GPI-anchored proteins (Schwartz et al., 2005).

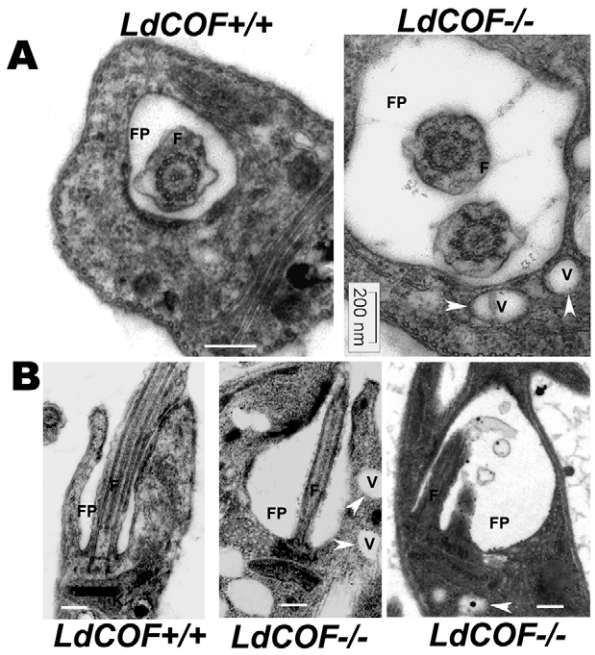

Fig. 5. Ultrastructural abnormalities in the flagellar pocket of *COF*$^{-/-}$ cells. (**A**) Transmission electron micrographs of thin sections of chemically fixed whole cells through the flagellar-pocket region showing the presence of two flagella within a single enlarged flagellar pocket in *COF*$^{-/-}$ cells. In case of *COF*$^{+/+}$ cells, most of the cross sections revealed the presence of single flagellum within the flagellar pocket. Enlarged pockets and accumulation of membrane bound vesicles in the cytoplasm as well as close to the flagellar-pocket lumen may also be seen in cross sections of *COF*$^{-/-}$ cells. Arrowheads indicate the membrane-bound vesicles. Scale bar: 200 nm. (**B**) Longitudinal sections through the flagellar-pocket region showing enlargement of the flagellar pocket and the presence of two flagella in the same flagellar pocket in *COF*$^{-/-}$ cells. Arrowheads indicate the membrane-bound vesicles accumulated at the flagellar pocket region. F, flagellum; FP, flagellar pocket; V, vesicles; K, kinetoplast. Scale bars: 200 nm.

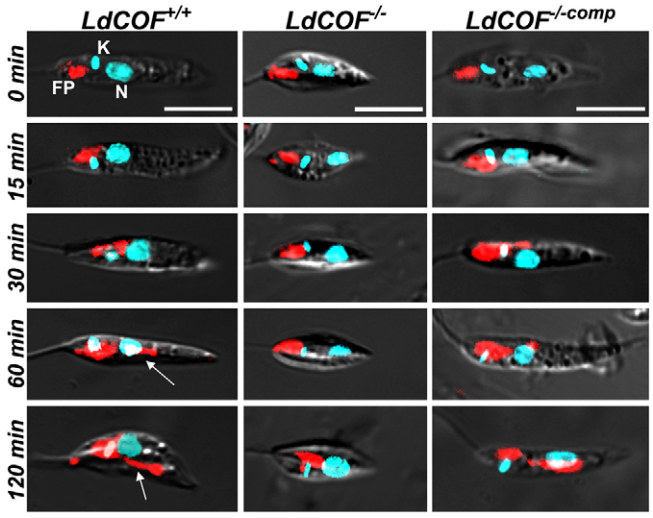

Fig. 6. Effect of *COF* gene disruption on vesicular trafficking. *COF*$^{+/+}$, *COF*$^{-/-}$ and *COF*$^{-/-\text{Comp}}$ cells were incubated with 2 µg/ml FM4-64 for 15 minutes at 4°C in dark. The cells were then incubated at 25°C and harvested at different time intervals and fixed by paraformaldehyde. DIC images (gray) were merged with Hoechst 33342 (cyan) and FM4-64 dye (red) for presentation. Arrows indicate the movement of dye to the posterior end of the cell. FP, flagellar pocket; N, nucleus; K, kinetoplast. Scale bars: 5 µm.

These trafficking events involve recycling of several important proteins, such as clathrin, GTPase and Rab proteins (Garcia-Salcedo et al., 2004; Field et al., 2007), maintaining the flagellar-pocket membrane in a highly dynamic state. Since the flagellar-pocket membrane is devoid of microtubule cytoskeleton, it is possible that actin, as the flagellar-pocket cytoskeleton, regulates various dynamic activities of this organelle, such as endocytosis and membrane-furrow formation, during cell division. This is well supported by our observations that *COF*-null cells show absence of actin localization at the apical region of their flagellar pockets and highly reduced actin dynamics, as well as an increased number of flagellar pockets containing two flagella, compared with the *COF*$^{+/+}$ and *COF*$^{-/-\text{Comp}}$ cells. Interestingly, despite the larger size of the flagellar pockets in the *COF*-null cells, the distances between the divided basal bodies are much smaller than in the wild-type cells, suggesting that the basal body separation is an active process, which requires the dynamic form of actin. Because, besides actin and Cof, myosin XXI is also present in the flagellar-pocket region (Katta et al., 2009), and because actin-based myosin motors essentially require the dynamic form of actin for their cellular activities (Zheng et al., 2009; Cramer, 2008; Semenova et al., 2008), we speculate that acto-myosin motor activity is involved in both basal body separation and vesicular trafficking in this organism.

In a closely related organism, *Trypanosoma*, it has been reported that ablation of flagellum formation results in short and immotile cells that fail to undergo cytokinesis, suggesting that the flagellum defines the position and direction of cleavage-furrow progression during cytokinesis (Kohl et al., 2003). Furthermore, ablation of flagellar biogenesis in these organisms has been shown to result in disturbances in flagellar-pocket organization (Absalon et al., 2008a). Flagellar elongation is essential for correct orientation and function of the flagellar pocket in these organisms (Absalon et al., 2008b). RNAi mutants of radial-spokes and central-pair proteins in *Trypanosoma* fail to undergo the final stage of cytokinesis, abscission, which leaves the daughter cells connected to each other at the posterior ends (Ralston et al., 2006; Branche et al., 2006), suggesting that the flagellar beating contributes the physical forces that are required to separate the daughter cells. Consistent with these observations, ablation of flagellar formation is accompanied by a reduction in cell growth in *Leishmania* cells (Cuvillier et al., 2000; Thiel et al., 2008; Tammana et al., 2008). However, it was hypothesized that because the *Leishmania* flagellum is mostly free from the cell body, a similar role to that of the *Trypanosoma* flagellum might not be expected (Kohl et al., 2003). This is supported by an earlier study which showed that the mutants of a dynein isoform (*DHC2.2*) in *L. mexicana* possess short flagella, but do not show any growth reduction (Adhiambo et al., 2005). Moreover, we did not observe any arrest of cell division at the abscission stage in *Leishmania* Cof mutants. Unlike in *Trypanosoma*, cytokinesis in these mutants proceeded more slowly than in the wild-type cells, but without any serious problems. Given these significant differences in cellular organization, a direct role of the flagellum in the *Leishmania* cell division can be ruled out at present.

It is intriguing to note that despite the completion of karyokinesis and formation of the microtubule septum, the daughter cells are still not separated. In trypanosomatids, the corset microtubules are

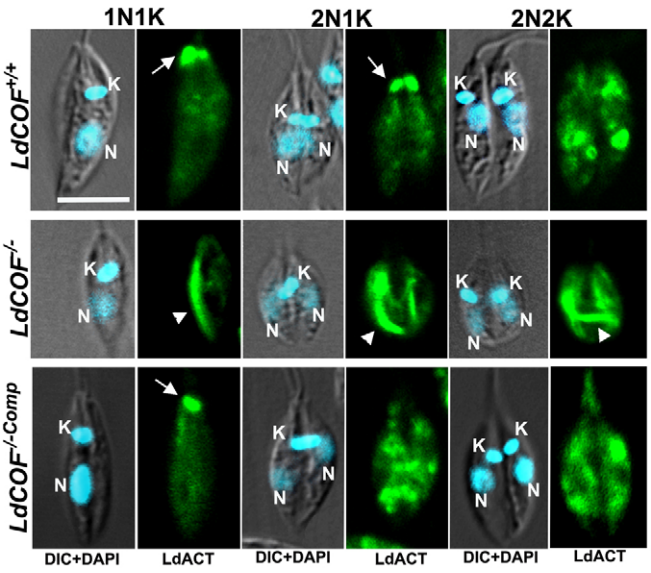

Fig. 7. Cell-cycle-dependant distribution of actin in cells labeled with antibodies against *Leishmania* actin. Immunofluorescence images show the enrichment of actin at the anterior tip of the flagellar pocket (arrows) during the initial biflagellate stage of the cell division in $COF^{+/+}$ and $COF^{-/-Comp}$ cells. Redistribution of actin in these cells was observed at the later stages of cytokinesis. In case of $COF^{-/-}$ cells, most of the cellular actin is sequestered in the form of long cables in the cell body (arrowheads). Continuous extension of actin cables into the daughter cells can also be seen in dividing $COF^{-/-}$ cells. DIC images (gray) are merged with DAPI (cyan) images showing nucleus and kinetoplast. LdACT, *Leishmania* actin; N, nucleus; K, kinetoplast. Scale bar: 5 µm.

closely associated with the pellicular membrane (Gull, 1999). Therefore, the membrane ingression would need to follow an 'interlocking-zipper' mechanism along the cleavage-furrow microtubules from the anterior to the posterior end, up to the abscission stage to facilitate daughter-cell separation. Our results show that the cell division in Cof-null cells is arrested at the early stage of cytokinesis that includes flagellar-pocket division and cleavage-furrow formation. Although, no link between these two processes has so far been established, both these processes should require remodeling of the flagellar-pocket membrane. Apparently, this remodeling relies on the dynamic action of the actin network, and is delayed if the network is disrupted. During *Leishmania* cytokinesis, stages between the furrow formation and daughter-cell separation are so fast that the intermediate stages are rarely observed in culture. Interestingly, most of the Cof-null cells are arrested in the furrow-ingression stage and no dividing cells are encountered at the subsequent stages (i.e. after the furrow ingression and before the stage of abscission), indicating that once the furrow ingression is initiated, subsequent stages do not face any problem and the daughter cells separate normally. These results reveal that the actin dynamics is required only to trigger the initiation of furrow formation and is not involved in the downstream events during cytokinesis.

The process of membrane remodeling includes the addition of several specific proteins and lipids to the existing membrane, which in association with underlying cytoskeletal elements acquire different shapes and curvatures. The actin cytoskeleton has long been known to remodel the plasma membrane during various cellular processes, for example, formation of pseudopods or ruffles and cytokinetic furrows. During furrow formation, endocytic vesicles have been reported to serve as a pool of proteins and other membrane components in the mammalian cells (Barr and Gruneberg, 2007). This is consistent with our present observation that slower trafficking of endocytic vesicles, which is primarily caused by the impaired actin dynamics, is associated with delayed cleavage furrow formation in Cof-null cells. That actin in trypanosomatids is involved in intracellular vesicular trafficking and flagellar-pocket organization is further supported by an earlier study which showed that loss of actin prevents endocytosis and results in enlargement of the flagellar pocket in the bloodstream form of *T. brucei* (Garcia-Salcedo et al., 2004). However, it is important to mention here that the *Leishmania* F-actin by itself displays fast dynamics compared with conventional actins (Kapoor et al., 2008), and therefore some monomeric actin is always available to drive the actin dynamics, although at a reduced pace, even in the absence of any actin-dynamics-regulating protein. It

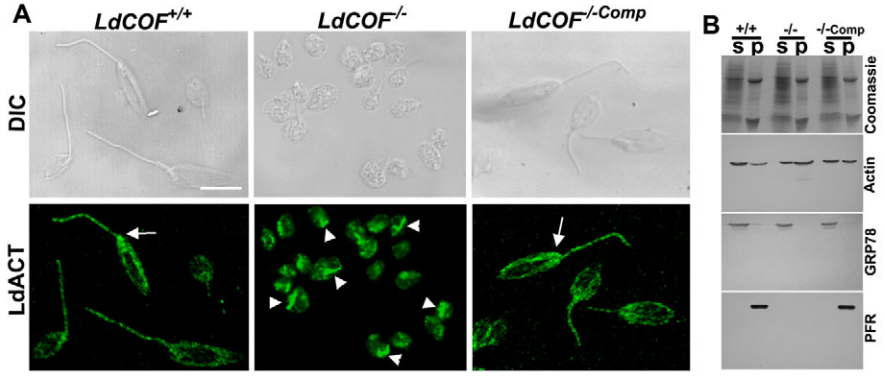

Fig. 8. Altered actin dynamics and cytoskeletal retention of actin in $COF^{-/-}$ cells. (**A**) Immunofluorescence images of cytoskeletons prepared by treatment of $COF^{+/+}$, $COF^{-/-}$ and $COF^{-/-Comp}$ cells with 0.5% NP-40. The cytoskeletons were stained with anti-*Leishmania* actin antibodies (LdACT). $COF^{-/-}$ cells appear short and stumpy compared with long and slender $COF^{+/+}$ cells (Tammana et al., 2008). Arrows indicate the presence of actin at the flagellar pocket region in $COF^{+/+}$ and $COF^{-/-Comp}$ cells. Arrowheads represent the retention of actin cables in the $COF^{-/-}$ cells. LdACT, *Leishmania* actin (green). Scale bar: 5 µm. (**B**) Western blot analysis of cytoskeletal retention of actin in $COF^{+/+}$, $COF^{-/-}$ and $COF^{-/-Comp}$ cells using antibodies against *Leishmania* actin. Anti-GRP78 (glucose-regulated protein of 78 kDa molecular mass) and anti-PFR antibodies were used as marker proteins for soluble and pellet fractions, respectively. +/+, $COF^{+/+}$ cells; –/–, $COF^{-/-}$ cells; *–/–Comp*, $COF^{-/-Comp}$ cells; s, soluble fraction; p, pellet fraction.

might therefore be visualized that deletion of the *Leishmania COF* gene has only slowed down, but not abolished, the dynamics of filamentous actin, which has resulted only in the slowing down of the actin-based processes. This suitably accounts for the delayed flagellar-pocket division and impairment of the vesicular trafficking in $COF^{-/-}$ cells.

The cell cycle events of trypanosomatids broadly follow the general eukaryotic model, except that several checkpoints exist in these organisms (Woodward and Gull, 1990; Ploubidou et al., 1999). Defects in cytokinesis do not necessarily trigger mitotic checkpoints, as a result of which cells continue DNA replication and become multinucleated as a result of cytokinetic block (Ploubidou et al., 1999). However, we could not observe any multinucleated cells in the $COF^{-/-}$ cell population despite a delay in cytokinesis, suggesting an arrest of further nuclear division, as well as stimulation of the cell cycle block. Similar cytokinetic arrest has been observed in BILBO1 RNAi *T. brucei* cells, which results in apparent mitotic block (Bonhivers et al., 2008). The presence of significant numbers of undivided flagellar pockets in dividing $COF^{-/-}$ cells suggests that the flagellar-pocket division acts as a control point before daughter cell separation. Aberrations in flagellar-pocket separation trigger mitosis checkpoints, which results in a block of karyokinesis in the arrested cells. These results thus indicate that flagellar-pocket division has an important role in the *Leishmania* cell-division cycle. Finally, very little is known about the proteins that regulate the various steps involved in *Leishmania* cytokinesis (Hammarton et al., 2007). The results presented in this study show that ADF/cofilin-driven F-actin dynamics facilitates early events in *Leishmania* cell division.

Materials and Methods

Leishmania cultures and growth-curve analysis

Leishmania donovani $COF^{+/+}$ cells were maintained in high-glucose DMEM supplemented with 10% heat-inactivated fetal bovine serum (FBS) and 40 mg/l gentamicin at 25°C. $COF^{-/-}$ cells were grown in the same medium in the presence of 50 μg/ml G418 and 50 μg/ml hygromycin B and $COF^{-/-Comp}$ cells (Tammana et al., 2008) were also grown in the same medium in the presence of 10 μg/ml tunicamycin. For growth analysis, $COF^{+/+}$, $COF^{-/-}$ and $COF^{-/-Comp}$ cells were grown in DMEM containing 10% fetal calf serum (FCS) without any antibiotics. Initially, the cells were seeded at a density of 1×10^6 cells/ml and the number of cells was counted at 24 hour time intervals with a Neubauer hemocytometer.

Cof-null mutants and $COF^{-/-Comp}$ cells

Leishmania $COF^{-/-}$ cells were generated through sequential targeted replacement of the ADF/cofilin gene by selective marker genes conferring resistance to neomycin or hygromycin by site-specific homologous recombination, essentially as described earlier (Tammana et al., 2008). For the generation of $COF^{-/-Comp}$ cells, we transfected the $COF^{-/-}$ cells with plasmid p6.5MCS containing the full-length *COF* gene tagged with GFP at its N-terminus (*p6.5GFP-COF*) and the transfected cells were selected on DMEM agar plates containing 10 μg/ml tunicamycin, as described earlier (Tammana et al., 2008).

Cell cycle analysis

For flow cytometry analysis, cells were fixed as described (Dvorak, 1993) with slight modification. Briefly, about 10^7 cells from $COF^{+/+}$, $COF^{-/-}$ and $COF^{-/-Comp}$ cultures (asynchronous) were centrifuged separately at 3000 r.p.m. for 5 minutes, washed with cold PBS and resuspended in 50 μl phosphate-buffered saline (PBS) (pH 7.2). The cell suspension was mixed with 150 μl of fixative solution (1% Triton X-100, 40 mM citric acid, 20 mM sodium phosphate, 200 mM sucrose) and incubated at room temperature for 5 minutes. Finally, 350 μl of diluent buffer (125 mM $MgCl_2$ in PBS) was added and the samples were stored at 4°C until further use. The fixed cells were treated with 50 μg RNase (5 mg/ml in 0.2 M sodium phosphate buffer, pH 7.0) for 3 hours at 37°C. Then, 50 μg/ml propidium iodide (5 mg/ml in 1.12% sodium citrate) was added and the tubes were incubated at 25°C for 1 hour. The samples were left overnight for equilibration at 4°C. The samples were analyzed on a FACS Calibur (Becton Dickinson), and the proportions of G1, S and G2-M populations were determined using ModFit software. Around 20,000 events were collected for each sample. For synchronization experiments, cells were maintained in exponential growth phase ($\leq10^7$ cells/ml). About 1×10^7 cells/ml were centrifuged and transferred into fresh DMEM containing 200 μg/ml hydroxyurea and incubated at 25°C for 12 hours. The cells were washed twice with PBS and resuspended in fresh DMEM containing 10% FCS without hydroxyurea. Aliquots were taken at regular time intervals and the samples were processed for FACS analysis after addition of propidium iodide as described above.

Fluorescence microscopy

The nuclear and kinetoplast configurations of the cells were analyzed by staining the cells with 4′,6-diamidino-2-phenylindole (DAPI). Briefly, cells from $COF^{+/+}$, $COF^{-/-}$ and $COF^{-/-Comp}$ asynchronous and synchronous cultures were centrifuged separately and washed with cold PBS twice and attached to poly-L-lysine (0.01% solution)-coated glass coverslips. The cells were fixed with 4% paraformaldehyde for 30 minutes at room temperature and washed thoroughly with PBS. The fixed cells were permeabilized with 0.5% Triton X-100 for 10 minutes at room temperature and washed twice with PBS. The coverslips were mounted using Fluorescein-FragEL mounting medium (Calbiochem) containing DAPI and analyzed on a Leica DM 5000B fluorescence microscope using ×63 1.4 NA (oil) Plan Apochromat lens. The cell configurations were categorized into 1N1K, 2N2K, 2N1K depending on the number of nuclei and kinetoplasts per cell and the percentage of each category was quantified.

For flagellar-pocket analysis, synchronized $COF^{+/+}$, $COF^{-/-}$ and $COF^{-/-Comp}$ cells were stained with ConA-rhodamine essentially as described earlier (Moraes et al., 2008). Briefly, cells were washed twice with cold PBS and fixed with 4% paraformaldehyde for 30 minutes at room temperature. The fixed cells were washed three times with cold PBS, resuspended in 1 ml PBS and then treated with 1:500 dilution of ConA-rhodamine (1 mg/ml in PBS) for 2 hours at room temperature. The cells were subsequently washed twice with PBS to remove excess ConA-rhodamine and then attached to poly-L-lysine (0.01% solution)-coated glass coverslips. The coverslips were mounted using Fluorescein-FragEL mounting medium (Calbiochem) containing DAPI and images were captured on a Zeiss LSM510 META confocal microscope using a ×63 1.4 NA (oil) Plan Apochromat lens.

Immunofluorescence microscopy of synchronized cultures of $COF^{+/+}$, $COF^{-/-}$ and $COF^{-/-Comp}$ cells was performed as described earlier (Tammana et al., 2008). *Leishmania* actin and Cof antibodies were prepared following our published procedure (Sahasrabuddhe et al., 2004; Tammana et al., 2008) and anti-α-tubulin and anti-β-tubulin antibodies were procured from Sigma. The primary antibodies were used in combination with appropriate Alexa Fluor 488-conjugated goat anti-mouse secondary antibodies (Molecular Probes, 1:1000) and Cy3-conjugated goat anti-rabbit secondary antibodies (Sigma, 1:1000). Images were captured on a Zeiss LSM510 META Confocal Microscope using a ×63 1.4 NA (oil) Plan Apochromat lens. The specificity of anti-*Leishmania* actin antibodies has been established and reported by us earlier (Nayak et al., 2005; Sahasrabudde et al., 2004).

Transmission electron microscopy

Transmission electron microscopic analysis of $COF^{+/+}$, $COF^{-/-}$and $COF^{-/-Comp}$ cells was performed essentially as described earlier (Tammana et al., 2008).

Intracellular vesicular trafficking

For monitoring vesicular trafficking activity, internalization of FM4-64 was performed essentially as described (Sahin et al., 2008). Briefly, 10^7/ml exponentially growing cells were incubated in DMEM containing 10% FCS and 2 μg/ml FM4-64 (Molecular Probes) dye was added and the mixture incubated at 4°C for 15 minutes and thereafter the temperature was raised to 25°C. Small aliquots (50 μl) were harvested at different time intervals and mixed with 2% paraformaldehyde solution in PBS. To the fixed labeled cells was added Hoechst 33342 dye at 10 μg/ml concentration and the cells were immediately imaged under Zeiss LSM510 META confocal microscope using a ×63 1.4 NA (oil) Plan Apochromat lens and 3× digital zoom.

Cytoskeleton preparation

Leishmania promastigote cytoskeletons from $COF^{+/+}$, $COF^{-/-}$ and $COF^{-/-Comp}$ cells were prepared essentially as described earlier (Nayak et al., 2005) and analyzed by western blotting and immunofluorescence microscopy. Briefly, equal number of cells (about 10^8) of each sample were pelleted at 4°C and washed twice with chilled PBS. The washed cells were treated with 0.5% NP40 solution in PBS at 4°C for 5 minutes, and then centrifuged at 12,000 r.p.m. at 4°C. The soluble and pellet fractions were separated on polyacrylamide gels (10%) by electrophoresis and analyzed by western blotting using anti-*Leishmania* actin, anti-GRP78 and anti-PFR (mAb2E10) antibodies. mAb2E10 and GRP78 antibodies were a kind gift from Diane McMahon Pratt (Yale University, CT) and Emanuela Handman (Walter and Eliza Hall Institute of Medical Research, Melbourne, Australia), respectively. For immunofluorescence microscopy, the cytoskeletons were allowed to settle on poly-L-lysine-coated glass coverslips and processed for labeling as described above.

This work was partially supported from a research grant to C.M.G. by the Department of Biotechnology, Government of India, New Delhi (India) under the Distinguished Biotechnology Research Professorship Award Scheme. Funding from Council of Scientific and Industrial Research (grant NWP0038) is also acknowledged. T.V.S.T. is a recipient

of Senior Research Fellowship from Council of Scientific and Industrial Research, New Delhi (India). We are grateful to A. L. Vishwakarma for his help with FACS analysis. This is communication No. 7719 from CDRI, Lucknow (India).

Supplementary material available online at
http://jcs.biologists.org/cgi/content/full/123/11/1894/DC1

References

Abe, H., Obinata, T., Minamide, L. S. and Bamburg, J. R. (1996). *Xenopus laevis* actin-depolymerizing factor/cofilin: a phosphorylation-regulated protein essential for development. *J. Cell Biol.* **132**, 871-885.

Absalon, S., Blisnick, T., Kohl, L., Toutirais, G., Doré, G., Julkowska, D., Tavenet, A. and Bastin, P. (2008a). Intraflagellar transport and functional analysis of genes required for flagellum formation in trypanosomes. *Mol. Biol. Cell* **19**, 929-944.

Absalon, S., Blisnick, T., Bonhivers, M., Kohl, L., Cayet, N., Toutirais, G., Buisson, J., Robinson, D. and Bastin, P. (2008b). Flagellum elongation is required for correct structure, orientation and function of the flagellar pocket in *Trypanosoma brucei*. *J. Cell Sci.* **121**, 3704-3716.

Adhiambo, C., Forney, J. D., Asai, D. J. and LeBowitz, J. H. (2005). The two cytoplasmic dynein-2 isoforms in *Leishmania mexicana* perform separate functions. *Mol. Bichem. Parasitol*. **143**, 216-225.

Aizawa, H., Sutoh, K., Tsubuki, S., Kawashima, S., Ishii, A. and Yahara, I. (1995). Identification, characterisation and intracellular distribution of cofilin in *Dictyostelium discoideum*. *J. Biol. Chem.* **270**, 10923-10932.

Allen, M. L., Dobrowolski, J. M., Muller, H., Sibley, L. D. and Mansour, T. E. (1997). Cloning and characterization of actin depolymerising factor from *Toxoplasma gondii*. *Mol. Biochem. Parasitol.* **88**, 43-52.

Barr, F. A. and Gruneberg, U. (2007). Cytokinesis: placing and making the final cut. *Cell* **131**, 847-860.

Blanchoin, L. and Pollard, T. D. (1998). Mechanism of interaction of *Acanthamoeba* actophorin (ADF/Cofilin) with actin filaments. *J. Biol. Chem.* **274**, 15538-15546.

Bonhivers, M., Nowacki, S., Landrein, N. and Robinson, D. R. (2008). Biogenesis of the trypanosome endo-exocytotic organelle is cytoskeleton mediated. *PLoS Biol.* **6**, 1033-1046.

Branche, C., Kohl, L., Toutirais, G., Buisson, J., Cosson, J. and Bastin, P. (2006). Conserved and specific functions of axoneme components in trypanosome motility. *J. Cell Sci.* **119**, 3443-3455.

Carlier, M. F., Laurent, V., Santolini, J., Melki, R., Didry, D., Xia, G. X., Hong, Y., Chua, N.-H. and Pantaloni, D. (1997). Actin depolymerizing factor (ADF/ cofilin) enhances the rate of filament turnover: implications in actin based motility. *J. Cell Biol.* **136**, 1307-1322.

Cramer, L. (2008). Organelle transport: dynamic actin tracks for myosin motors. *Curr. Biol*. **18**, 1066-1068.

Cuvillier, A., Radon, F., Antoine, J. C., Chardin, P., De Vos, T. and Merlin, G. (2000). LdARL-3A, a *Leishmania* promastigotes-specific ADP-ribosylation factor-like protein, is essential for flagellar intergrity. *J. Cell Sci.* **13**, 2065-2074.

Desjeux, P. (2004). Leishmaniasis: current situation and new perspectives. *Comp. Immunol. Microbiol. Infect. Dis.* **27**, 305-318.

Dvorak, J. A. (1993). Analysis of the DNA of parasitic protozoa by flow cytometry. In *Methods in Molecular Biology. Protocols in Molecular Parasitology* (ed. J. E. Hyde), pp. 191-204. Totowa: Humana Press Inc.

Field, M. C., Natesan, S. K., Gabernet-Castello, C. and Koumandou, V. L. (2007). Intracellular trafficking in the trypanosomatids. *Traffic* **8**, 629-639.

Garcia-Salcedo, J. A., Perez-Morga, D., Gijon, P., Dilbeck, V., Pays, E. and Nolan, D. P. (2004). A differential role for actin during the life cycle of *Trypanosoma brucei*. *EMBO J.* **23**, 780-789.

Gull, K. (1999). The cytoskeleton of trypanosomatid parasites. *Annu. Rev. Microbiol.* **53**, 629-655.

Gunsalus, K. C., Bonaccorsi, S., Williams, E., Verni, F., Gatti, M. and Goldberg, M. L. (1995). Mutations in twinstar, a drosophila gene encoding a Cofilin/ADF homologue, results in defects in centrosome migration and cytokinesis. *J. Cell Biol.* **131**, 1243-1259.

Hammarton, T. C., Monnerat, S. and Mottram, J. C. (2007). Cytokinesis in trypanosomatids. *Curr. Opin. Microbiol.* **10**, 520-527.

Kapoor, P., Sahasrabuddhe, A. A., Kumar, A., Mitra, K., Siddiqui, M. I. and Gupta, C. M. (2008). An unconventional form of actin in protozoan hemoflagellate *Leishmania*. *J. Biol. Chem.* **283**, 22760-22773.

Katta, S. S., Sahasrabuddhe, A. A. and Gupta, C. M. (2009). Flagellar localization of a novel isoform of myosin, myosin XXI, in *Leishmania*. *Mol. Biochem. Parasitol.* **164**, 105-110.

Kohl, L., Robinson, D. and Bastin, P. (2003). Novel roles for the flagellum in cell morphogenesis and cytokinesis of trypanosomes. *EMBO J.* **22**, 5336-5346.

Kunda, P. and Baum, B. (2009). The actin cytoskeleton in spindle assembly and positioning. *Trends Cell Biol.* **19**, 174-179.

Lacomble, S., Vaughan, S., Gadelha, C., Morphew, M. K., Shaw, M. K., McIntosh, J. R. and Gull, K. (2009). Three-dimensional cellular architecture of the flagellar pocket and associated cytoskeleton in trypanosomes revealed by electron microscope tomography. *J. Cell Sci*. **122**, 1081-1090.

Morgan, G. W., Hall, B. S., Denny, P. W., Carrington, M. and Field, M. C. (2002a). The kinetoplastida endocytic apparatus. Part I: A dynamic system for nutrition and evasion of host defences. *Trends Parasitol.* **18**, 491-496.

Morgan, G. W., Hall, B. S., Denny, P. W., Field, M. C. and Carrington, M. (2002b). The endocytic apparatus of the kinetoplastida. Part II: Machinery and components of the system. *Trends Parasitol*. **18**, 540-546.

Moraes, C. S., Seabra, S. H., Castro, D. P., Brazil, R. P., de Souza, W., Garcia, E. S. and Azambuja, P. (2008). *Leishmania* (*Leishmania*) *chagasi* interactions with *Serratia marcescens*: ultrastructural studies, lysis and carbohydrate effects. *Exp. Parasitol.* **118**, 561-568.

Mullin, K. A., Foth, B. J., Ilgoutz, S. C., Callaghan, J. M., Zawadzki, J. L., McFadden, G. I. and McConville, M. J. (2001). Regulated degradation of an endoplasmic reticulum membrane protein in a tubular lysosome in *Leishmania mexicana*. *Mol. Biol. Cell.* **12**, 2364-2377.

Nayak, R. C., Sahasrabuddhe, A. A., Bajpai, V. K. and Gupta, C. M. (2005). A novel homologue of coronin colocalizes with actin in filament-like structures in *Leishmania*. *Mol. Biochem. Parasitol.* **143**, 152-164.

Ono, S. (2007). Mechanism of depolymerization and severing of actin filaments and its significance in cytoskeletal dynamics. *Int. Rev. Cytol.* **258**, 1-82.

Ono, K., Parast, M., Alberico, C., Benian, G. M. and Ono, S. (2003). Specific requirement for two ADF/cofilin isoforms in distinct actin-dependent processes in *Caenorhabditis elegans*. *J. Cell Sci*. **116**, 2073-2085.

Ploubidou, A., Robinson, D. R., Docherty, R. C., Ogbadoyi, E. O. and Gull, K. (1999). Evidence for novel cell cycle checkpoints in trypanosomes: kinetoplast segregation and cytokinesis in the absence of mitosis. *J. Cell Sci.* **112**, 4641-4650.

Pollard, T. D. and Borisy, G. G. (2003). Cellular motility driven by assembly and disassembly of actin filaments. *Cell* **112**, 453-465.

Qualmann, B. and Kessels, M. M. (2009). New players in actin polymerization-WH2-domain-containing actin nucleators. *Trends Cell Biol.* **19**, 276-285.

Ralston, K. S. and Hill, K. L. (2008). The flagellum of *Trypanosoma brucei*: new tricks from an old dog. *Int. J. Parasitol.* **38**, 869-884.

Ralston, K. S., Lerner, A. G., Diener, D. R. and Hill, K. L. (2006). Flagellar motility contributes to cytokinesis in Trypanosoma brucei and is modulated by an evolutionarily conserved dynein regulatory system. *Eukaryotic Cell* **5**, 696-711.

Robinson, D. R., Ogbadoyi, E. and Gull, K. (2003). A trans-membrane, high order structural linkage responsible for mitochondrial genome positioning and segregation by flagellar basal bodies in trypanosomes. *Mol. Biol. Cell* **14**, 1769-1779.

Sahasrabuddhe, A. A., Bajpai, V. K. and Gupta, C. M. (2004). A novel form of actin in *Leishmania*: molecular characterisation, subcellular localisation and association with subpellicular microtubules. *Mol. Biochem. Parasitol.* **134**, 105-114.

Sahasrabuddhe, A. A., Nayak, R. C. and Gupta, C. M. (2009). Ancient *Leishmania* coronin (CRN12) is involved in microtubule remodeling during cytokinesis. *J. Cell Sci*. **122**, 1691-1699.

Sahin, A., Espiau, B., Tetaud, E., Cuvillier, A., Lartigue, L., Ambit, A., Robinson, D. R. and Merlin, G. (2008). The *leishmania* ARL-1 and golgi traffic. *PLoS One* **20**, e1620.

Schuler, H., Mueller, A. K. and Matuschewski, K. (2005). A *Plasmodium* actin depolymerizing factor that binds exclusively to actin monomers. *Mol. Biol. Cell* **16**, 4013-4023.

Schwartz, K. J., Peck, R. F., Tazeh, N. N. and Bangs, J. D. (2005). GPI valence and the fate of secretory membrane proteins in African trypanosomes. *J. Cell Sci.* **118**, 5499-5511.

Semenova, I., Burakov, A., Berardone, N., Zaliapin, I., Slepchenko, B., Svitkina, T., Kashina, A. and Rodionov, V. (2008). Actin dynamics is essential for myosin-based transport of membrane organelles. *Curr. Biol.* **18**, 1581-1586.

Tammana, T. V. S., Sahasrabuddhe, A. A., Mitra, K., Bajpai, V. K. and Gupta, C. M. (2008). Actin-depolymerizing factor, ADF/cofilin, is essentially required in assembly of *Leishmania* flagellum. *Mol. Microbiol.* **70**, 837-852.

Thiel, M., Simon, H., Wiese, M., Kroemer, M. and Bruchhaus, I. (2008). Involvement of a *Leishmania* thymidine kinase in flagellum formation, promastigote shape and growth as well as virulence. *Mol. Biochem. Parasitol.* **158**, 152-162.

Van Troys, M., Huyck, L., Leyman, S., Dhaese, S., Vandekerkhove, J. and Ampe, C. (2008). Ins and outs of ADF/cofilin activity and regulation. *Eur. J. Cell Biol.* **87**, 649-667.

Waller, R. F. and Mc Conville, M. J. (2002). Developmental changes in lysosome morphology and function *Leishmania* parasites. *Int. J. Parasitol.* **32**, 1435-1445.

Woodward, R. and Gull, K. (1990). Timing of nuclear and kinetoplast DNA replication and early morphological events in the cell cycle of *Trypanosoma brucei*. *J. Cell Sci.* **95**, 49-57.

Zheng, M., Beck, M., Müller, J., Chen, T., Wang, X., Wang, F., Wang, Q., Wang, Y., Baluska, F., Logan, D. C. et al. (2009). Actin turnover is required for myosin-dependent mitochondrial movements in *Arabidopsis* root hairs. *PloS One* **4**, e5961.